# 6

# Chapter 6

## Slip Flow and Heat Transition for Hydromagnetic Elastico-Viscous Fluid Past a Flat Moving Plate

### 6.1 Introduction

Modern technology and industrial industries rely heavily on heat transfer mechanisms on moving solid surfaces for processes as diverse as liquid film extrusion, paper manufacture, plastic sheet extrusion, polymer industry, crystal development, and many more. The boundary layer flow behaviour for a solid moving plate at a constant velocity was investigated by Sakaidis [108]. The effects of suction and blowing on the transfer of heat and mass over a moving surface were studied by Erickson *et al.* [109]. Tsou *et al.* [110] undertook a theoretical analysis of the aforementioned issues for a continuously moving plate, then tested their findings experimentally. Over a moving plate, Rashidi *et al.* [111] offer a hydromagnetic mixed convective fluid flow with a partial slip boundary. Bhatti *et al.* [112] offer a collection of related issues on a shifting boundary under a variety of physical circumstances.

Many scientists have looked at fluid issues in which there is no slip condition across the boundary of a solid surface. Slip condition was first ignored, but it was subsequently

recognised that this assumption was incorrect for many real-world issues. The chemical cleansing and polishing procedure in medicine often exhibits the fluid flow with slip state. With a flat surface and a partial slide impact, Martin and Boyd [113] showed how heat may be transported on the boundary layer fluid. The radiation effect with momentum slip for unstable hydromagnetic boundary flow was studied by Pal *et al.* [114]. Hydromagnetic and slip effects on boundary layer fluid flow across a flat porous plate were established by Bhattacharyya *et al.* [115].

Furthermore, magnetohydrodynamic fluid flow and heat transfer across a moving flat surface have several current technical applications, such as those in petroleum engineering, geothermal energy, plasma research, aerodynamics, and many others. In addition, there are a wide variety of applications where several artificial techniques have been devised to govern behaviour or research the boundary layer. Free convective heat transfer for an isothermal plate caused by a magnetic field was studied by Sparrow and Cess [116]. For a moving wall with an electrically conducting vertical flow, Gupta [117] investigated the heat flux induced by the magnetic field. Newtonian fluid flow across a stretched surface governed by a momentum slip boundary condition was reported by Andersson [118] and Wang [119]. Numerous researchers have examined the possibility of hall impact for hydromagnetic boundary fluid flow across a revolving flat plate [120, 121].

The current investigation is motivated by the aforementioned publications, and seeks to examine the effects of hydromagnetic and slip on heat transfer for an elastic-viscous fluid flowing past a flat, moving plate using Walters's Liquid (Model $B'$). The MATLAB 'bvp4c' built-in solver is used to solve the reduced-form partial differential equations that govern fluid motion through similarity variables. Plots of the numerically analysed findings for varying values of the flow dominating parameters and other relevant flow feature parameters are shown and discussed.

## 6.2 Mathematical Formulation

Considering hydromagnetic and slip effects, we analyse the steady flow of a two-dimensional elastico-viscous boundary layer fluid through a flat, moving plate. Figure 6.1 depicts the model's flow geometry. Equations of motion for the governing fluid, taking account of the approximation theory of the boundary layer are:

$$\frac{\partial \mathrm{u}}{\partial \mathrm{x}} + \frac{\partial \mathrm{v}}{\partial \mathrm{y}} = 0 \qquad (6.2.1)$$

$$u\frac{\partial u}{\partial x}+v\frac{\partial u}{\partial y}=\nu\frac{\partial^2 u}{\partial y^2}-\frac{k_0}{\rho}\left[u\frac{\partial^3 u}{\partial x\,\partial y^2}+v\frac{\partial^3 u}{\partial y^3}-\frac{\partial u}{\partial y}\frac{\partial^2 u}{\partial x\,\partial y}-\frac{\partial v}{\partial y}\frac{\partial^2 u}{\partial y^2}\right]-\frac{\sigma {B_0}^2 u}{\rho} \quad (6.2.2)$$

$$u\frac{\partial T}{\partial x}+v\frac{\partial T}{\partial y}=\frac{K}{\rho C_p}\frac{\partial^2 T}{\partial y^2} \quad (6.2.3)$$

where,

u: velocity towards x-axis, v: velocity towards y- axis, $\nu=\frac{\mu}{\rho}$: kinematic viscosity,

$\mu$: fluid viscosity coefficient, $\rho$: fluid density, σ : fluid's electrical conductivity

$B_0$: magnetic field, $k_0$: elastic-viscous parameter, T: temperature,

K: fluid thermal conductivity, $C_p$: specific heat.

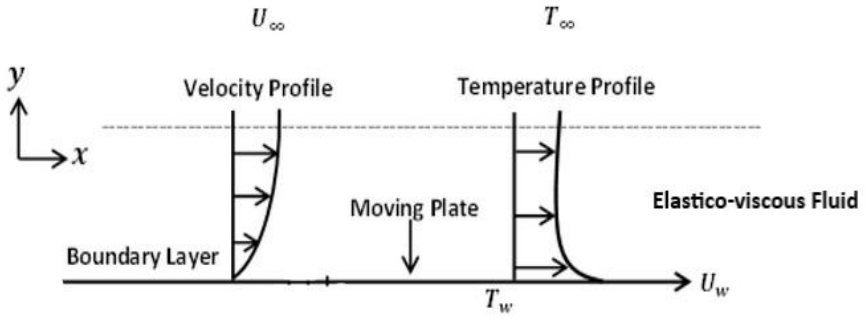


**Fig. 6.1** The flow geometry of the problem

The appropriate conditions imposed at the boundary:

$$u=U_w+A\left(\frac{\partial u}{\partial y}\right), v=0 \text{ at } y=0;\quad u\to U_\infty \text{ as } y\to\infty \quad (6.2.4)$$

$$T=T_w \text{ at } y=0\ ;\ T\to T_\infty \text{ as } y\to\infty \quad (6.2.5)$$

where, $U_w$: constant free velocity of the plate, $U_\infty$: constant free stream velocity,

A: Slip length, $T_w$: constant plate temperature, $T_\infty$: constant free stream temperature

Stream functions along with similarity variables taken as:

$$\Psi=\sqrt{2U_\infty \nu x}\,h(\eta), \eta=\sqrt{\frac{U_\infty}{2\nu x}}\,y, u=\frac{\partial \Psi}{\partial y}, v=-\frac{\partial \Psi}{\partial x}, T=T_w+(T_w-T_\infty)\theta(\eta) \quad (6.2.6)$$

Using the relation (6.2.6) in (6.2.2) and (6.2.3), we finally obtain the following sets of equation:

$$h'''(\eta)+h(\eta)h''(\eta)+k_1\left[2h'(\eta)h'''(\eta)+h(\eta)h^{v}(\eta)-\left(h''(\eta)\right)^2\right]+Mh'(\eta)=0 \quad (6.2.7)$$

$$\theta''(\eta)+Prh(\eta)\theta'(\eta)=0 \quad (6.2.8)$$

where $M=\frac{2x\sigma {B_0}^2}{\rho U_\infty}$: hydromagnetic parameter, $k_1=\frac{k_0 U_\infty}{2\mu x}$: elastic-viscous parameter,

$Pr=\frac{\mu C_p}{K}$ : Prandtl number,

The final form of conditions imposed at the boundary obtained from (6.2.4) and (6.2.5) are:

$h(\eta) = 0,\ h'(\eta) = \lambda + \alpha h''(\eta)\ at\ \eta = 0\ ;\qquad h'(\eta) = 1,\ h''(\eta) = 0\ as\ \eta \to \infty$ (6.2.9)

$\theta(\eta) = 1\ at\ \eta = 0\ ;\ \theta(\eta) = 0\ as\ \eta \to \infty$ (6.2.10)

where, $\lambda = \frac{U_w}{U_\infty}$ : velocity ratio at the plate, $\alpha = \sqrt{\frac{U_\infty}{2\mu x}}$ : velocity slip parameter.

## 6.3 Method of Solution

The self-similar differential equations (6.2.7) and (6.2.8) are transformed to first order differential equations as:

$h = h_1, h' = h_2,\ h'' = h_3, h''' = h_4\ , \theta = h_5, \theta' = h_6$ (6.3.1)

From (6.3.1), we can write

$h_1' = h_2, h_2' = h_3, h_3' = h_4, h_5' = h_6,$ (6.3.2)

Making use of (6.3.1) and (6.3.2), the equations (6.2.7) and (6.2.8) can be written as:

$h_4' = \frac{1}{h_1}\left[(h_3)^2 - 2h_2h_4 - \left(\frac{1}{k_1}\right)\{h_4 + h_1h_3 + Mh_2\}\right]$ (6.3.3)

$f_6' = -Prh_1h_6$ (6.3.4)

and the applicable boundary conditions (6.2.9) and (6.2.10) reduces as follows:

$h_1(0) = 0, h_2(0) = \lambda + \alpha h_3(0)\ and\ \ h_2(\infty) = 1, h_3(\infty) = 0$ (6.3.5)

$h_5(0) = 1\ \ and\ \ h_5(\infty) = 0$ (6.3.6)

## 6.4 Results and Discussion

Using the built-in MATLAB programme "bvp4c," the numerical calculation of the results of velocity profile and temperature profiles are shown in order to determine the physical relevance of the flow pattern for each of the included flow parameters. The findings are shown graphically in Figs. 6.2 to 6.9 by varying factors such as elastico-viscous $k_1$, hydromagnetic M, Velocity ratio λ, slip α and the Prandtl number Pr. The velocity ratio parameter is considered to be smaller than 1 in this study.

The velocity profile $h'(\eta)$ for change of $k_1$, M, λ and α against $\eta$ is shown in Figs. 6.2 to 6.4. Fig. 6.2 illustrates how fluid transmission improves initially as $k_1$ grows, eventually declines as distance increases, and then settles down. Fluid flow improves initially as temperature in the fluid aids in deforming the polymers of elastic-viscous material, but as distance increases, the benefits of temperature eventually diminish and the fluid motion is

slowed. According to Fig. 6.3, the fluid motion initially decreases as M increases, but at $\eta = 2$ and higher, it begins to accelerate for some distance before eventually slowing down with uniform flow. The Lorentz force, which is produced by magnetic fields, initially resists fluid motion, but as it travels further, its impact lessens, causing fluid velocity to increase briefly before eventually settling.

It can be seen from Fig. 6.4 that the velocity increases with a significant variance in the curves at first due to rising values of α, and subsequently the velocity decreases and ultimately settles down with no deviations. The outcome is completely justified since the slip parameter aids in fluid moving freely at the plate, but as distance increases, more fluid stores up at the plate and the slip factor's benefits weaken. With the rising of λ, the velocity first decelerates then progressively increases for a time until ultimately levelling out with distance, as shown in Fig. 6.5. Physically, this may be explained as an increase in the velocity ratio parameter, a fall in free stream velocity, and a subsequent decrease in fluid velocity that quickly settles down.

Figs. 6.6 to 6.9 show the temperature profile $\theta(\eta)$ with the variation of $k_1$, M, Pr and λ against $\eta$. According to Fig. 6.6, the fluid gets more viscous as $k_1$ increases, which prevents thermal energy from being transferred to the fluid readily and causes temperature curves to decline. From Fig. 6.7, it is noticed that the fluid temperature is not greatly impacted by the rising values of M. It is evident from Figs. 6.8 and 6.9 that the temperature of the fluid decreased as Pr and λ grew. The outcome is acceptable since increasing Pr reduces the fluid's heat conductivity. As the velocity ratio parameter increases, the free stream velocity drops and less heat is transferred from the plate to the fluid. The findings indicate that the medium and flow factors affect the fluid's temperature.

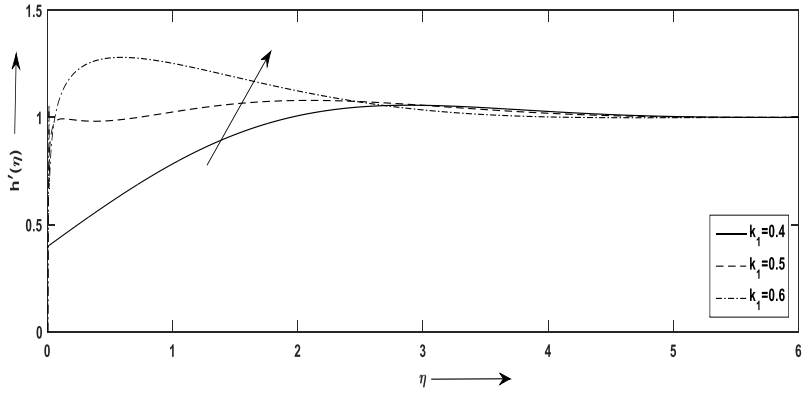


**Fig. 6.2** Velocity $h'(\eta)$ versus $\eta$ for $k_1$ with $M = 0.1$, *λ=0.1, α=0.3, Pr=0.4*

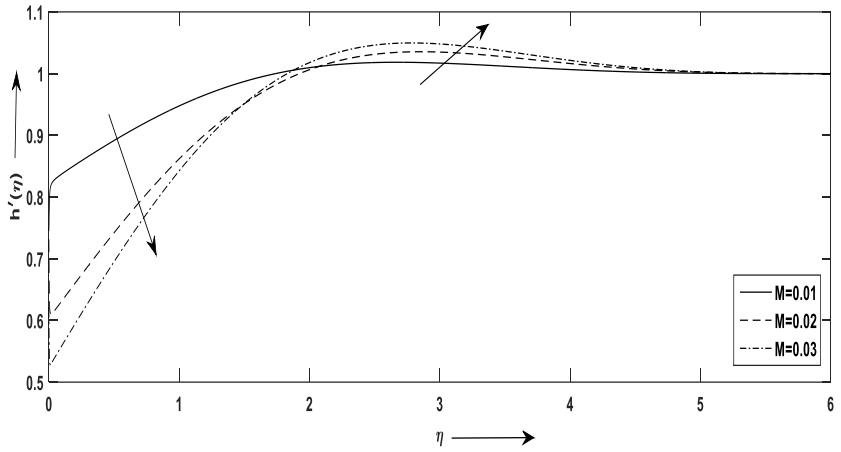


**Fig. 6.3** Velocity $h'(\eta)$ versus $\eta$ for M with$k_1 = 0.4$, *λ=0.1, α=0.3, Pr=0.4*

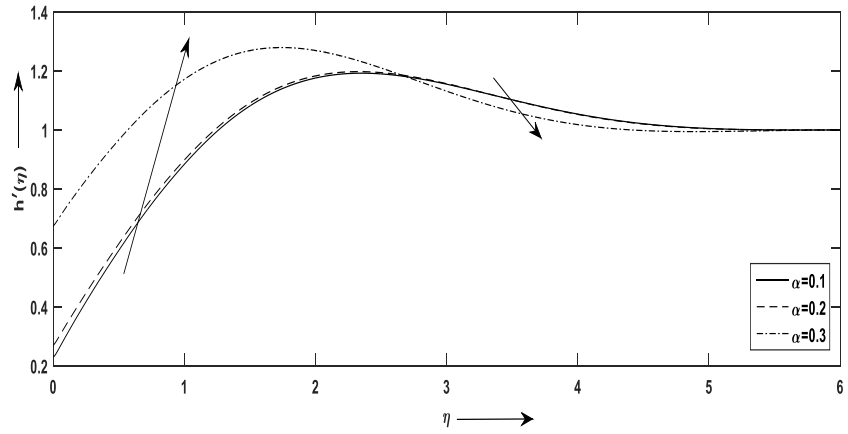


**Fig.6.4** Velocity $h'(\eta)$ versus $\eta$ for α with $k_1 = 0.4$, *M=0.1, λ=0.1, Pr=0.4*

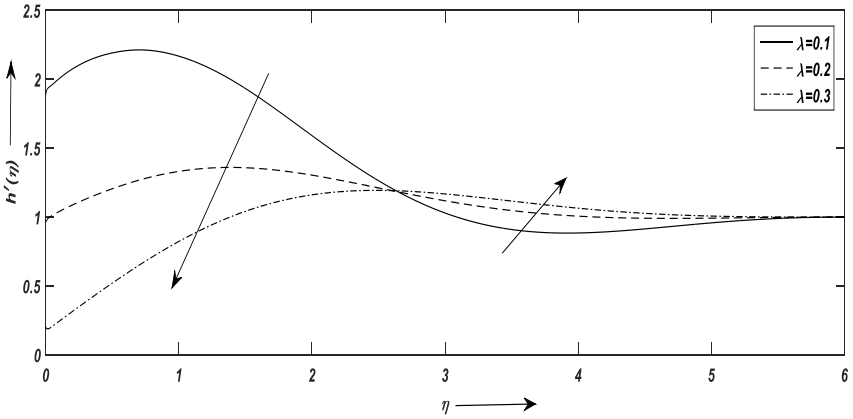


**Fig.6.5** Velocity $h'(\eta)$ versus $\eta$ for λ with $k_1 = 0.4$, *M=0.1, α=0.3, Pr=0.4*

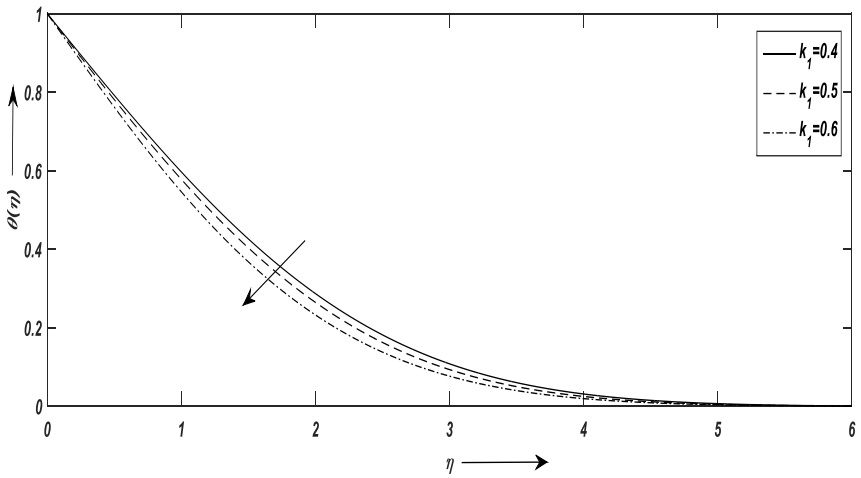


**Fig. 6.6** Temperature $\theta(\eta)$ versus $\eta$ for $k_1$ with *M=0.1, α=0.3, λ=0.1, Pr=0*

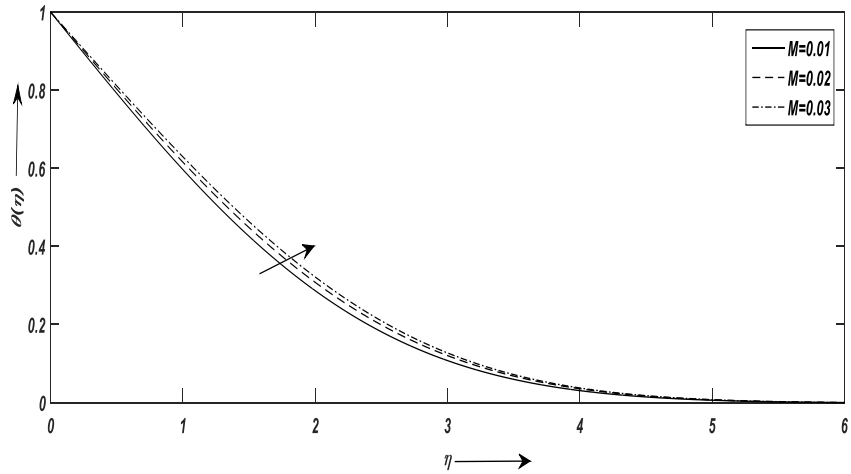


**Fig. 6.7** Temperature $\theta(\eta)$ versus $\eta$ for *M*

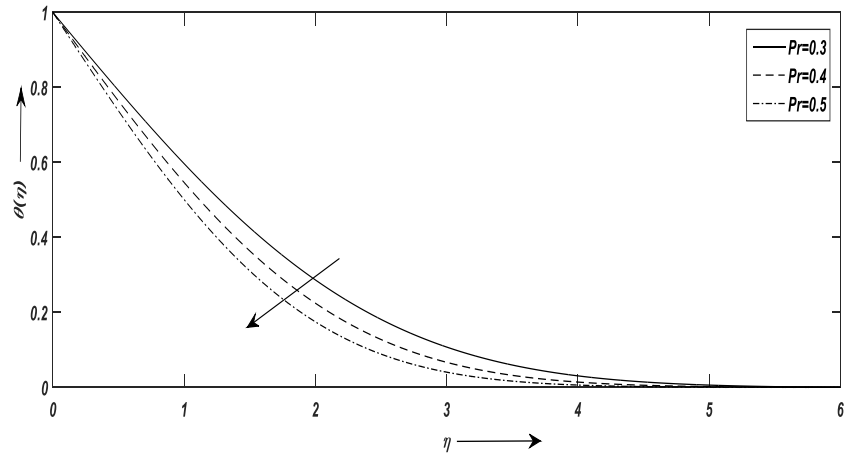


**Fig. 6.8** Temperature $\theta(\eta)$ versus $\eta$ for $Pr$ with $k_1$*=0.4, M=0.1 α=0.3, λ=0.1*

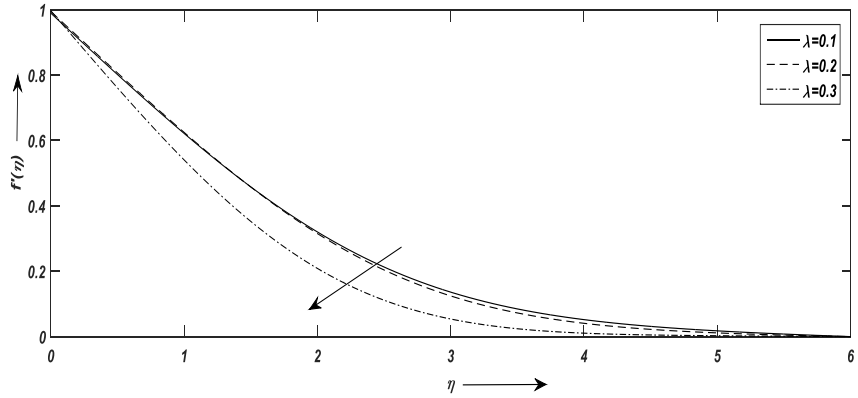


**Fig. 6.9** Temperature $\theta(\eta)$ versus $\eta$ for λ with $k_1$=*0.4, M=0.1 α=0.3, Pr=0.4*

## 6.5 Conclusion

This research looked at how hydromagnetic fields and slip affect the temperature change in an elastic-viscous boundary layer as it flows past a moving flat plate. The resulting equations of fluid motion are solved using the MATLAB software 'bvp4c,' which is based on the finite difference approach. In other words, this work may be developed further. It is possible to compare the outcomes of several analytical and numerical approaches. Flow simulation of the issue may be performed to provide a good view of the outcomes.

The study's findings may be summed up as follows.:

- At first, a rise in fluid temperature helps to deform polymers of elastico-viscous material, resulting in increased fluid flow; but, as the fluid moves farther away from its source, its temperature decreases, slowing the fluid's motion.
- The magnetic field creates a resistive force that at first opposes the motion of the fluid, but with increasing distance, its impact diminishes and the fluid velocity increases for a time before settling down.
- The slip parameter allows fluid to flow more freely at the plate, but its benefits diminish as more fluid accumulates at the plate over time.
- As the velocity ratio parameter increases, the free stream velocity drops, resulting in a gradual slowing and eventual settling of the fluid velocity.
- The increase in elastic viscosity renders the fluid more viscous, which hinders the transfer of thermal energy to the fluid, resulting in a drop in temperature curves.
- As the Prandtl number grows the thermal conductivity of the fluid falls.
- The growth of the velocity ratio parameter lowers the free-stream velocity and, consequently, the heat transfer from the plate to the fluid.